

Field-Induced Transition in the $S=1$ Antiferromagnetic Chain with Single-Ion Anisotropy in a Transverse Magnetic Field

Huaizhong Xing,¹ Gang Su,^{2,*} Song Gao³, and Junhao Chu¹

¹*National Laboratory for Infrared Physics, Shanghai Institute of Technical Physics, Chinese Academy of Sciences, Shanghai 200083, China*

²*Department of Physics, The Graduate School of the Chinese Academy of Sciences, P.O. Box 3908, Beijing 100039, China*

³*State Key Laboratory of Rare Earth Materials Chemistry and Applications, PKU-HKU Joint Laboratory on Rare Earth Materials and Bioinorganic Chemistry, Peking University, Beijing 100871, China*

Abstract

The field-induced transition in one-dimensional $S = 1$ Heisenberg antiferromagnet with single-ion anisotropy in the presence of a transverse magnetic field is obtained on the basis of the Schwinger boson mean-field theory. The behaviors of the specific heat and susceptibility as functions of temperature as well as the applied transverse field are explored, which are found to be different from the results obtained under a longitudinal field. The anomalies of the specific heat at low temperatures, which might be an indicative of a field-induced transition from a Luttinger liquid phase to an ordered phase, are explicitly uncovered under the transverse field. A schematic phase diagram is proposed. The theoretical results are compared with experimental observations.

PACS Numbers: 75.50.Ee, 75.30.Gw, 75.40.Cx

I. INTRODUCTION

The study on one-dimensional (1D) magnetic systems began in 1930's.¹ Although several decades passed, the low-dimensional antiferromagnets have still received much renewed attention owing to both experimental and theoretical efforts in the past few years. On the theoretical aspect, most recent works associated with methods such as finite-size scaling,³ numerical calculations,^{4,5} Monte Carlo methods,⁶ analyses of an exactly solvable model,⁷ etc., have been devoted to verifying Haldane's conjecture² that the uniform integer spin chain with Heisenberg antiferromagnetic interactions is massive whereas the half-integer spin chain is massless, and much progress towards understanding Haldane's scenario has been made so far.

On the other hand, Haldane's conjecture has been confirmed experimentally in a number of 1D antiferromagnets with spin integer. Quite recently, Honda et al^{8,9} reported an anomaly of heat capacity on a single crystal sample of the $S = 1$ quasi-1D Heisenberg antiferromagnet (HAF) $Ni(C_5H_{14}N_2)_2N_3(PF_6)$ (briefly NDMAP) in applied magnetic fields, and identified such an anomaly as an indication of a field-induced magnetic long-range ordering. They found an anisotropy in the susceptibility which can be explained as due to the single-ion anisotropy of Ni^{2+} . The model Hamiltonian they adopted is expressed as

$$H = J \sum_{\langle ij \rangle} \mathbf{S}_i \cdot \mathbf{S}_j + D \sum_i (S_i^z)^2 - \mu_B \sum_i \mathbf{S}_i \cdot \tilde{\mathbf{g}} \cdot \mathbf{h} \quad (1)$$

where J is the exchange integral (for NDMAP $J/k_B \sim 30K$), D is the single-ion anisotropy constant, μ_B is the Bohr magneton, and $\tilde{\mathbf{g}}$ is the g tensor with elements g_{\perp} and g_{\parallel} corresponding to the g values perpendicular and parallel to the chain c axis, respectively.

Motivated by this nice experiment, we have recently discussed such an 1D system in a longitudinal magnetic field.¹⁰ As this magnetic system is expected to reveal quite different behaviors in longitudinal and transverse applied fields, as manifested by experiments^{8,9}, it would be interesting to pay attention to the case in a transverse magnetic field. It is thus the purpose of this present article to report thermodynamic behaviors of this system in the presence of a transverse magnetic field by means of the modified Schwinger boson mean-field theory (SBMFT). As is well known, the SBMFT works well for the 1D HAF with integer spins, which can include the effects of quantum fluctuations self-consistently in the large- N saddle point, where N is the quasiparticle degeneracy. The Schwinger boson approach is actually a large- N formulation, and the large- N limit of Hamiltonian is taken with $\kappa = n_b/N$ fixed^{12,13,14} with the constraint $b^+b = n_b$ at each site for Schwinger bosons. For large values of κ the system is magnetically ordered in high dimensions, while the quantum disordered state appears at small κ . In the presence of a magnetic field one may expect the degeneracy to be lifted and N could be smaller than in the absence of a magnetic field. By noting that the degeneracy is for Schwinger boson quasiparticles, the SBMFT still works even if the applied magnetic field lifts some degeneracies, because even for small N it is known that the SBMFT can produce fair results for the 1D HAF with integer spin (see, e.g. Ref.[12]). Our so-obtained results would thus be reliable at the mean-field level.

The outline of this paper is as follows. In next section, the thermodynamic quantities such as the specific heat and the transverse susceptibility will be calculated based on the framework of the SBMFT. The detail formalism of SBMFT for this present system is collected in the Appendix. Finally, a summary and discussion will be presented.

II. THERMODYNAMIC PROPERTIES AT FINITE TEMPERATURES

Based on the self-consistent equations developed in the Appendix, we may obtain the static uniform transverse susceptibility (along x direction) per site by

$$\begin{aligned} \chi/2N = & \frac{\mu_B^2 g_\perp^2}{2N} \sum_k \left\{ \beta \frac{U^2(k)}{1 - U^2(k)} \{ [n_\alpha(k) + 1]n_\alpha(k) + [n_\beta(k) + 1]n_\beta(k) \} \right. \\ & \left. + \frac{(1 - U^2(k))^{-\frac{3}{2}}}{2\Lambda'} (n_\alpha(k) + n_\beta(k) + 1) \right\}, \end{aligned} \quad (2)$$

where

$$U(k) = \eta\gamma_k - \frac{\mu_B g_\perp h_x}{2\Lambda'}, \quad n_{\alpha(\beta)}(k) = \frac{1}{e^{\beta E_k^{\alpha(\beta)}} - 1}. \quad (3)$$

The specific heat per site, $C/2N$, can be easily obtained by $\frac{C(T)}{2N} = \frac{1}{2N} \frac{\partial E}{\partial T}$, where E is the internal energy. For convenience in numerical calculations, we shall set $J = 1$ as energy scale, $g_\perp = 2.17$ (from Ref. [8]) and $k_B = 1$ hereafter.

A. Specific Heat

The temperature dependence of the specific heat (C_v) for different fields at $D = 0$ is shown as in Fig. 1. One may see that the specific heat increases with increasing field at low temperature, whereas it decreases with increasing field at high temperature. At a given magnetic field $0 < h_x < 0.9$, there is an anomaly clearly observed in the curve of C_v at a temperature T_c . If the transverse field is taken off, the anomaly disappears. Such an anomaly might be an indicative of field-induced transition. Recall that in the presence of a longitudinal field, the system shows no any anomaly in the curve of C_v observed.¹⁰ In this sense, this kind of field-induced transition appears only when a transverse magnetic field is applied to the system within the framework of the SBMFT. By noting that the anomalies were also observed in experiments for different longitudinal fields at almost the same temperature, although with smaller peaks than applying the transverse fields. The fact that our SBMFT cannot produce this result shows that there might be some limitations for this approach. With increasing the magnetic field, the temperature T_c where the field-induced transition occurs, moves to low temperature side. Combining the results of susceptibility (see below), we may identify the transition as one from a disordered phase to a spin-polarized phase. We could understand this phenomenon as a consequence of the broken of the Z_2 symmetry.¹⁶ When the external field is applied along the z -axis, the XY symmetry is retained. On the contrary, when the magnetic field is applied perpendicularly to the z -axis, the XY symmetry is broken and an Ising anisotropy is produced (See, e.g. Ref. [8] and references therein). At a given field an anomaly of specific heat will thus appear at a given temperature due to the Z_2 symmetry breaking, which is an indicative of a field-induced transition from a disordered phase to a spin-polarized phase as the transverse field tends to align spins perpendicular to the easy axis. Here we would like to point out that the anomaly we observed is different from the usual broad peak of C_v which appears at temperature T_p whatever the magnetic field is present or absent, while T_p decreases with increasing the field. Since the limitation of

the approximation we cannot find such a broad peak of C_v within the frame of SBMFT, as discussed in a number of references. This may be a shortcoming of the SBMFT. However, at high temperature we have observed the specific heat decreases with increasing the field, which shows a correct trend for $S = 1$ AFM chain. On the other hand, we note that the anomalies in the curves of C_v were observed experimentally for NDMAP at high magnetic fields. Our calculated result is in qualitatively agreement with this experimental observation⁸ if we make a rescale for the field as $h_x \rightarrow (h_c - h_x)$,¹⁹ where h_c is a critical field at which the anomaly of specific heat disappears at zero temperature. In the present case $h_c \approx 0.90$. With this field rescaling, we find that the temperature where the anomaly occurs increases with the field, consistent with the experimental observation. We would like to point out that we could not compare the experimental data directly with our calculated results, because the experimental data⁸ include the contribution of the lattice which is not given. However, one may see that the results obtained on the basis of the SBMFT in the present fashion might capture qualitatively some experimental features of the $S = 1$ HAF chain in the presence of a transverse field. Besides, our SBMFT result seems also to be in qualitatively agreement with the upper phase boundary of the exact diagonalization of finite chains, although the latter results are extracted from the staggered susceptibility.¹⁶

We have also investigated the effect of the single-ion anisotropy on the specific heat in a given field $h_x = 0.3$, as shown in Fig. 2. The result shows that the anisotropy does not have so much effect on the specific heat, and it only causes slight changes in the peaks and dips of C_v . It appears that C_v increases, though small, with increasing D , as indicated in the inset of Fig. 2. One may notice that this result is very different from the case in the presence of a longitudinal applied field, where the effect of the single-ion anisotropy on specific heat is various.¹⁰ This result is readily understandable, because the single-ion anisotropy is XY-like, and if the magnetic field is applied perpendicular to the z -axis, the single-ion anisotropy would have no much effect on the physical observables, as illustrated in the present case, while such an anisotropy would matter if the magnetic field is applied along the z -axis, as manifested in Ref.[10].

The external field dependence of the specific heat for different temperatures at $D = 1.0$ is depicted in Fig. 3. It is shown that at a given temperature the specific heat increases with increasing field, and after arriving at a maximum, decreases faster and then slow with increasing field. One may see again that there are anomalies in the curves of the specific heat versus the external field. It is interesting to note that the magnetic field at which the specific heat shows a peak at a given temperature is consistent with those found in Fig. 1. For a given temperature, $C_v(h_x)$ behaves as $C_v(h_x) \sim c_0(T) + c_1(T)h_x^{1/2} + c_2(T)h_x + c_3(T)h_x^{3/2}$, where c_i ($i = 0, 1, 2, 3$) are temperature-dependent coefficients. For example, at $T = 0.5$ the fitting results give $c_0 = 0.1643, c_1 = 0.7013, c_2 = -1.2047, c_3 = 0.468$. At $h_x \rightarrow 0, C(T = 0.5)$ is 0.1643. It can be seen that after making a field rescaling $h_x \rightarrow h_c - h_x$ one may find that the position of the anomaly of the specific heat moves to high field side with increasing temperature.

B. Transverse Susceptibility

The temperature dependence of susceptibility (χ) at $D = 1.0$ in different fields is depicted in Fig. 4. It is observed that the susceptibility shows a broad peak at low temperature in

low fields (in our case $h_x < 0.485$), which is a characteristic of $S = 1$ Heisenberg AFM chain, and it goes to zero at $T \rightarrow 0$ for the field less than $h_{c1} = 0.485$, suggesting that the system is in a Haldane gapped phase in this regime. For $0.485 < h_x < 0.9$, we found the susceptibility of this 1D spin system goes to a finite value as T tends to zero, implying that in this regime the system is in a Luttinger liquid (LL) phase. It is clear that there exists a transition from the Haldane gapped phase to the LL phase at $h_x = h_{c1}$ at which the excited gap closes. The result agrees with that of the effective-field theory and size scaling analysis¹⁸ with the finite chain calculation^{19,20}, which indicates that the field-induced transition occurs from the disordered ground state to the gapless Tomonaga-Luttinger liquid phase at some critical external field h_{c1} . In addition, a phase boundary in field (h_{c1})-temperature (T) plane is thus obtained by observing the variation of susceptibility. On the other hand, for $h_{c1} < h < h_{c2}$, the gap vanishes and we find a range of linear T dependence for the specific heat, which is also a characteristic for the LL phase.^{21,22} For the higher field ($h_x \geq h_{c2} = 0.9$) the susceptibility diverges and persists up to saturation as temperature tends to zero, showing that the system now enters into a spin-polarized phase. Thus, there must be a transition from the LL phase to a spin-polarized phase at $h_x = h_{c2}$. However, it is not easy to determine h_{c2} according to the divergence of the susceptibility. Fortunately, we observed that there is a curvature change in the curves of χ versus temperature for different fields, as enlarged in the inset of Fig. 4. Although the curvature change in the susceptibility itself is not an indication of a phase transition, by observing that the susceptibility shows different behaviors at low temperatures in different phases, one could identify when the system enters into the spin-polarized phase from the LL phase by observing the curvature change of the susceptibility. The positions of curvature change are the same as the positions in curves of the specific heat at which the specific heat exhibits an anomaly, which gives the estimation of h_{c2} . In other words, at h_{c2} the specific heat shows anomalies, indicating a transition occurs at h_{c2} . Note that the curvature-changing position moves to low temperature side with increasing field. It can be observed that the behavior of susceptibility in the transverse field is very different from the results in the longitudinal field,¹⁰ where there is no curvature-changing observed in the curves of χ versus temperature.

The effect of the single-ion anisotropy on susceptibility is also investigated. It is found that the single-ion anisotropy does not change so much the shape and the magnitude of susceptibility. Though the effect on susceptibility is not obvious, it can cause a small decreasing of χ at a given temperature and a given field. One can obtain a schematic phase diagram in field (h_x)-anisotropy (D) plane by observing the variation of susceptibility, as shown in Fig. 5. The phase boundary is characterized by closure of the excited gap. The system is in a gapless phase above the boundary and is in a gapped Haldane phase below the boundary. One may note that the change of h_x with D in the diagram is only a few percent. Whatever the anisotropy is strong or weak, the system is always in the Haldane phase if h_x is less than 0.45. When D is larger, the external field required to drive the system into the gapless phase becomes larger. For example, at $D = 0$, the critical field is 0.45, and at $D = 1.6$, it becomes 0.50. It is found that the critical field in the case of the transverse field is larger than that in the longitudinal field. For instance, at $D = 0$ and $T \rightarrow 0$ the critical field in the transverse case is 0.45, while it is 0.155 in the longitudinal case. Our result is in agreement with the estimation on the critical field at $D = 0$ on the basis of exact diagonalization of finite chains,¹⁶ and is qualitatively consistent with the experimental

extrapolation in NDMAP⁸.

Fig. 6 gives the field-dependence of susceptibility at $D = 1.0$ at different temperatures. It is observed that for $h_x < 0.9$ the behavior of χ versus transverse field at low temperature is quite different from that at high temperature. The positions of curvature change in χ are consistent with our observation for the anomalies in specific heat. We also observed that the single-ion anisotropy does not have much effect on the behavior of the susceptibility versus transverse field.

III. SUMMARY AND DISCUSSION

By summarizing the above results on the specific heat and the susceptibility, we may propose a schematic phase diagram in field (h_x)-temperature (T) plane within the framework of SBMFT. Since the anisotropy does not have much effect on the behavior of thermodynamic observables of the system under interest, without loss of generality we present the phase diagram for $D = 0$ as an example, as shown in Fig. 7. When the transverse field is less than h_{c1} , the system should be in a gapped phase (Haldane phase). At $h_x = h_{c1}$ the gap closes. The lower boundary for h_{c1} is determined by observing the closure of spin gap in the curves of the susceptibility as a function of the applied transverse field and temperature. For $h_x < h_{c2}$, the system might be in a Luttinger liquid phase, characterized by finite values of the susceptibility at $T \rightarrow 0$. When $h_x > h_{c2}$, the system goes into a spin-polarized phase. At $h_x = h_{c2}$, the anomalies in the curves of the specific heat as well as the susceptibility appear. It is interesting to observe that the shape of the LL phase becomes more symmetric for D nonzero. It seems that our proposed phase diagram based on the SBMFT is somewhat different from the results of exact diagonalization on finite chains.¹⁶ In the phase diagram presented in Ref. [16] the lower and upper boundaries of the antiferromagnetic ordered phase are given by h_{c1} and h_{c2} , which are determined by the staggered susceptibility. While in our proposed phase diagram, h_{c1} and h_{c2} are determined by observing the behaviors of the uniform transverse susceptibility as well as the specific heat. Considering the mean-field feature of our method, we cannot determine with accuracy whether a small region of an ordered phase at very low temperatures ($T < 0.1$) in the LL phase exists, as the susceptibility we calculated is not a staggered but uniform one. In this sense, our proposed phase diagram is not incompatible with that of Ref.[16], which can be viewed as a complement for finite-size calculations. Therefore, it could be better to understand the thermodynamic properties of this 1D spin system in the presence of the applied field based on a combination of our SBMFT results and finite-size calculations.

ACKNOWLEDGMENTS

This work is supported in part by the National Science Foundation of China (Grant No. 90103023 and 10104015), the State Key Project for Fundamental Research in China, and by the Chinese Academy of Sciences.

APPENDIX A: FORMALISM OF THE SBMFT

In this Appendix, we shall present the detail derivation of the self-consistent equations based on the SBMFT. These equations are applied to get the thermodynamic properties of the system.

We suppose that the system in Eq.(1) with $J > 0$ is defined on a bipartite lattice with sublattices A and B. For sublattice A, we denote the spin operator S_i^A by Schwinger bosons a_i and b_i (see Ref. [11]):

$$\begin{aligned} S_{i,+}^A &= -a_i^+ b_i^+, S_{i,-}^A = -a_i b_i, & i \in A \\ S_{i,z}^A &= \frac{1}{2}(a_i^+ a_i + b_i^+ b_i + 1), \end{aligned} \quad (A1)$$

satisfying the constraint $S_i^A = (a_i^+ a_i + b_i^+ b_i)$ for each site on sublattice A, and for sublattice B

$$\begin{aligned} S_{j,+}^B &= a_j b_j, S_{j,-}^B = a_j^+ b_j^+ & j \in B \\ S_{j,z}^B &= -\frac{1}{2}(b_j^+ b_j + a_j^+ a_j + 1) \end{aligned} \quad (A2)$$

with $S_j^B = (a_j^+ a_j + b_j^+ b_j)$ for each site on sublattice B. The bosons $\{a\}$ and $\{b\}$ obey the standard commutation relations. Although one may note that the definitions in Eqs. (2) and (3) introduced in Ref. [11] are slightly different from the standard form, we find that such a form is quite convenient for our purpose. On account of the definitions with constraints, the Hamiltonian (1) for $S = 1$ can be rewritten as

$$H = H_0 + H_D + H_{ex}, \quad (A3)$$

$$\begin{aligned} H_0 &= J \sum_{\langle i,j \rangle} \mathbf{S}_i \cdot \mathbf{S}_j = -2J \sum_{i=1,\delta} A_{i,i+\delta}^+ A_{i,i+\delta} \\ &\quad - J \sum_{i=1,\delta} a_i^+ a_i a_{i+\delta}^+ a_{i+\delta} + J \sum_{i=1,\delta} a_i^+ a_i, \end{aligned} \quad (A4)$$

$$H_D = D \sum_{i=1} (S_i^z)^2 = \frac{3D}{4} \sum_{i=1} (a_i^+ a_i + b_i^+ b_i) + DN/2, \quad (A5)$$

$$H_{ex} = -\mu_B \sum_i [g_{\perp} (S_i^x h_x + S_i^y h_y) + g_{\parallel} S_i^z h_z], \quad (A6)$$

where $A_{i,i+\delta} = \frac{1}{2}(a_i^+ b_{i+\delta}^+ + b_i a_{i+\delta})$, and $2N$ is the total number of sites. To implement the constraints $\sum_{i \in A} (a_i^+ a_i + b_i^+ b_i) = S^A$ and $\sum_{j \in B} (a_j^+ a_j + b_j^+ b_j) = S^B$ where $S^{A(B)}$ denotes the total spin of sublattice A(B), we should introduce two kinds of Lagrangian multipliers λ_i^A and λ_j^B into the system. At the mean-field level, for the sake of simplicity we may take the average value of the bond operator $\langle A_{i,i+\delta} \rangle = A$ to be uniform and static, and so are $\langle \lambda_i^A \rangle = \lambda^A$ and $\langle \lambda_j^B \rangle = \lambda^B$.

The mean-field Hamiltonian in momentum space reads

$$H = H_0 + H_D + H_{ex}, \quad (A7)$$

$$\begin{aligned}
H_0 = & -J \sum_k \{ A^* (a_{-k}^+ b_k^+ + b_k a_{-k}) z \gamma_k^* + (b_k a_{-k} + a_{-k}^+ b_k^+) z \gamma_k A \} \\
& - J \sum_k (\langle \tilde{n}_{i+\delta,a} \rangle a_{-k}^+ a_{-k} + \langle \tilde{n}_{i,a} \rangle a_{-k}^+ a_{-k}) \\
& + J \sum_k a_{-k}^+ a_{-k} + \lambda^A \sum_k [(a_{-k}^+ a_{-k} + b_k^+ b_k) - S^A] \\
& + \lambda^B \sum_k [(a_{-k}^+ a_{-k} + b_k^+ b_k) - S^B] \\
& + 2JzNA^*A + JNz \langle \tilde{n}_{i,a} \rangle \langle \tilde{n}_{i+1,a} \rangle,
\end{aligned} \tag{A8}$$

$$H_D = \frac{3D}{4} \sum_{i=1} (a_{-k}^+ a_{-k} + b_k^+ b_k) + DN/2, \tag{A9}$$

$$H_{ex} = -\frac{1}{2} \mu_B \sum_k [-g_{\perp} h_x (a_{-k}^+ b_k^+ + b_k a_{-k}) + \frac{-1}{j} g_{\perp} h_y (a_{-k}^+ b_k^+ - a_{-k} b_k) + g_{\parallel} h_z (a_{-k}^+ a_{-k} + b_k^+ b_k + 1)], \tag{A10}$$

where z is the number of nearest neighbor sites, j is a complex number, and $\gamma_k = \frac{1}{z} \sum_{\delta} e^{ik\delta} = \cos k$. The sum over k is restricted to the reduced first Brillouin zone.

Utilizing the Bogoliubov transformation

$$a_{-k} = \cosh \theta_k \alpha_k + \sinh \theta_k \beta_k^+, \quad b_k = \sinh \theta_k \alpha_k^+ + \cosh \theta_k \beta_k, \tag{A11}$$

with θ given by

$$\tanh 2\theta = \frac{-\mu_B g_{\perp} h_x + \text{Re}(2JzA\gamma_k)}{2\Lambda'}, \tag{A12}$$

with

$$2\Lambda' = (\lambda^A + \lambda^B) - B/2 + 3D/4, \quad B \equiv J[(\langle \tilde{n}_{i+1,a} \rangle + \langle \tilde{n}_{i,a} \rangle) - 1],$$

we obtain the energy spectrum of the system in the presence of a transverse external field $h_{ex} = (h_x, 0, 0)$:

$$E_k^{\alpha} = \sqrt{(2\Lambda')^2 - (2\text{Re}|JzA\gamma_k| - \mu_B g_{\perp} h_x)^2} - B/2, \tag{A13}$$

$$E_k^{\beta} = \sqrt{(2\Lambda')^2 - (2\text{Re}|JzA\gamma_k| - \mu_B g_{\perp} h_x)^2} + B/2. \tag{A14}$$

The free energy per site takes the form of

$$\begin{aligned}
\frac{F}{2N} = & \frac{1}{2N\beta} \sum_k \{ \ln[2 \sinh \frac{\beta}{2} (E_k^{\alpha})] + \ln[2 \sinh \frac{\beta}{2} (E_k^{\beta})] \} \\
& + JzA^*A + B/4 - (S^A/2 + 1/2)\lambda^A - \lambda^B(S^B/2 + 1/2) \\
& - D/2 + Jz \langle \tilde{n}_{i,a} \rangle \langle \tilde{n}_{i+1,a} \rangle / 2.
\end{aligned} \tag{A15}$$

The mean-field self-consistent equations can be obtained by minimizing the free energy. Without loss of generality, we may set $\lambda^A = \lambda^B$. Then, we perform $\delta F/\delta\lambda^A = 0$, $\delta F/\delta A^* = 0$, $\delta F/\delta \langle \tilde{n}_{i+\delta,a} \rangle = 0$ and $\delta F/\delta \langle \tilde{n}_{i,a} \rangle = 0$. Rescale the parameters $(\lambda^A, \lambda^B, A, \beta) \rightarrow (\Lambda, \eta, \kappa)$:

$$\eta = \frac{JAz}{\Lambda'}, \quad \beta = \frac{4\kappa}{z}. \quad (\text{A16})$$

Then, the angle in the Bogoliubov transformation can be expressed in a compact form

$$\cosh 2\theta_k = \frac{1}{\sqrt{1 - (\eta\gamma_k - \frac{\mu_B g_{\perp} h_x}{2\Lambda'})^2}}, \quad \sinh 2\theta_k = \frac{-\frac{\mu_B g_{\perp} h_x}{2\Lambda'} + \eta\gamma_k}{\sqrt{1 - (\eta\gamma_k - \frac{\mu_B g_{\perp} h_x}{2\Lambda'})^2}}. \quad (\text{A17})$$

The self-consistent equations become

$$(S^A + S^B)/2 + 1 = \frac{1}{2N} \sum_k \frac{1}{\sqrt{1 - (\eta\gamma_k - \frac{\mu_B g_{\perp} h_x}{2\Lambda'})^2}} \{ \coth \kappa (2\Lambda' \sqrt{1 - (\eta\gamma_k - \frac{\mu_B g_{\perp} h_x}{2\Lambda'})^2} + B/2) \\ + \coth \kappa (2\Lambda' \sqrt{1 - (\eta\gamma_k - \frac{\mu_B g_{\perp} h_x}{2\Lambda'})^2} - B/2) \}, \quad (\text{A18})$$

$$\Lambda' = \frac{1}{2N} \sum_k \frac{J\gamma_k}{\eta} \cdot \frac{-\frac{\mu_B g_{\perp} h_x}{2\Lambda'} + \eta\gamma_k}{\sqrt{1 - (\eta\gamma_k - \frac{\mu_B g_{\perp} h_x}{2\Lambda'})^2}} \{ \coth \kappa (2\Lambda' \sqrt{1 - (\eta\gamma_k - \frac{\mu_B g_{\perp} h_x}{2\Lambda'})^2} + B/2) \\ + \coth \kappa (2\Lambda' \sqrt{1 - (\eta\gamma_k - \frac{\mu_B g_{\perp} h_x}{2\Lambda'})^2} - B/2) \}, \quad (\text{A19})$$

$$4 < \tilde{n}_{i,a} > +1 = \\ \frac{1}{2N} \sum_k \{ \left[\frac{1}{\sqrt{1 - (\eta\gamma_k - \frac{\mu_B g_{\perp} h_x}{2\Lambda'})^2}} - 1 \right] \coth \kappa (2\Lambda' \sqrt{1 - (\eta\gamma_k - \frac{\mu_B g_{\perp} h_x}{2\Lambda'})^2} + B/2) \\ + \left[\frac{1}{\sqrt{1 - (\eta\gamma_k - \frac{\mu_B g_{\perp} h_x}{2\Lambda'})^2}} - 1 \right] \coth \kappa (2\Lambda' \sqrt{1 - (\eta\gamma_k - \frac{\mu_B g_{\perp} h_x}{2\Lambda'})^2} - B/2) \}, \quad (\text{A20})$$

$$4 < \tilde{n}_{i+1,a} > +1 = \\ \frac{1}{2N} \sum_k \{ \left[\frac{1}{\sqrt{1 - (\eta\gamma_k - \frac{\mu_B g_{\perp} h_x}{2\Lambda'})^2}} + 1 \right] \coth \kappa (2\Lambda' \sqrt{1 - (\eta\gamma_k - \frac{\mu_B g_{\perp} h_x}{2\Lambda'})^2} - B/2) \\ + \left[\frac{1}{\sqrt{1 - (\eta\gamma_k - \frac{\mu_B g_{\perp} h_x}{2\Lambda'})^2}} - 1 \right] \coth \kappa (2\Lambda' \sqrt{1 - (\eta\gamma_k - \frac{\mu_B g_{\perp} h_x}{2\Lambda'})^2} + B/2) \}. \quad (\text{A21})$$

As is easily seen, the aforementioned equations are highly coupled, and it is not possible to get useful analytic results. They are only solved numerically to get the relevant thermodynamic quantities.

REFERENCES

*Corresponding author. E-mail: gsu@gscas.ac.cn

- ¹ H. Bethe, Z. Phys. **71**, 205 (1931).
- ² F. D. M. Haldane, Phys. Lett. **93A**, 464 (1983); F. D. M. Haldane, Phys. Rev. Lett. **50**, 1153 (1983).
- ³ R. Botet and R. Jullien, Phys. Rev. B **27**, 613 (1983); R. Botet and R. Jullien and M. Kolb, *ibid.* **28**, 3914 (1983); M. Kolb, R. Botet and R. Jullien, J. Phys. A **16**, L673 (1983).
- ⁴ J. B. Parkinson and J. C. Bonner, Phys. Rev. B **32**, 4703 (1985).
- ⁵ T. Sakai and M. Takahashi, Phys. Rev. B **42**, 4573 (1990).
- ⁶ M. P. Nightingale and H. W. Blote, Phys. Rev. B **33**, 659 (1985).
- ⁷ I. Affleck, T. Kennedy, E. H. Lieb and H. Tasaki, Commun. Math. Phys. **115**, 477 (1988).
- ⁸ Z. Honda, H. Asakawa and K. Katsumata, Phys. Rev. Lett. **81**, 2566 (1998).
- ⁹ Z. Honda, K. Katsumata, H.A. Katori, K. Yamada, T. Oshishi, T. Manabe and M. Yamashita, J. Phys. Cond. Mat.: **9**, L83 (1997); *ibid* **9**, 3487 (1997).
- ¹⁰ G. Su, H. Xing, D. Xue, Z. Chen and F. Li, Inter. J. Mod. Phys. B **14**, 2561 (2000).
- ¹¹ D. C. Mattis, The Theory of Magnetism I (Springer-Verlag, Berlin, Heidelberg, 1965).
- ¹² D. P. Arovas and A. Auerbach, Phys. Rev. B **38**, 316 (1988); A. Auerbach, *Interacting Electrons and Quantum Magnetism* (Springer-Verlag, New York, 1994).
- ¹³ S. Sachdev and N. Read, Int. J. Mod. Phys. B **5**, 219 (1991).
- ¹⁴ N. Read and S. Sachdev, Phys. Rev. Lett. **66**, 1773 (1991).
- ¹⁵ S. Sachdev, Phys. Rev. B **45**, 12377 (1992).
- ¹⁶ T. Sakai, Phys. Rev. B **62**, R9240 (2000).
- ¹⁷ G. Chaboussant et al., Phys. Rev. Lett. **80**, 2713 (1998); H. Mayaffre et al., Phys. Rev. Lett. **85**, 4795 (2000).
- ¹⁸ I. Affleck, Phys. Rev. B **43**, 3215 (1991).
- ¹⁹ T. Sakai and M. Takahashi, Phys. Rev. B **43**, 13383 (1991).
- ²⁰ T. Sakai and M. Takahashi, J. Phys. Soc. Jpn. **60**, 3615 (1991).
- ²¹ H. Mayaffre et al., Phys. Rev. Lett. **85**, 4795 (2000).
- ²² X. Wang and L. Yu, Phys. Rev. Lett. **84**, 5399 (2000).

FIGURE CAPTIONS

Fig. 1 The temperature dependence of the specific heat at $D = 0$ for different transverse fields.

Fig. 2 The temperature dependence of the specific heat for different anisotropies at $h_x = 0.3$. Inset: The enlarged part of the specific heat versus temperature for different anisotropies at $h_x = 0.3$.

Fig. 3 The h_x -dependence of the specific heat at $D = 1.0$ for different temperatures.

Fig. 4 The temperature dependence of the susceptibility at $D = 1.0$ for different transverse fields. Inset: The enlarged part of the susceptibility versus temperature at $D = 1.0$ for different transverse fields.

Fig. 5 Schematic phase diagram in $h_x - D$ plane. The solid line is the phase boundary on which the gap closes.

Fig. 6 The h_x -dependence of the susceptibility at $D = 1.0$ for different temperatures.

Fig. 7 Schematic phase diagram in $h_x - T$ plane.

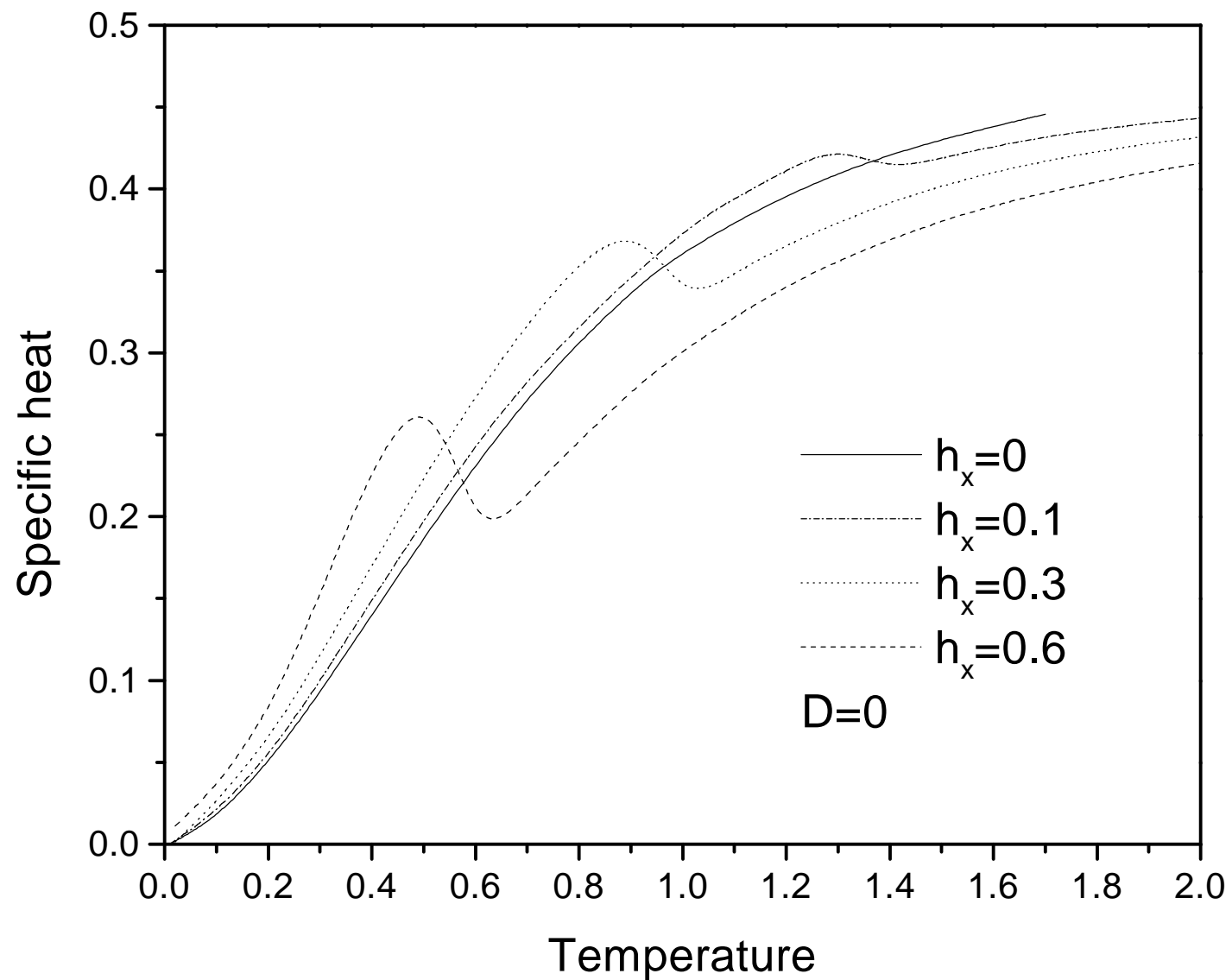


Fig.1 Xing, Su et al

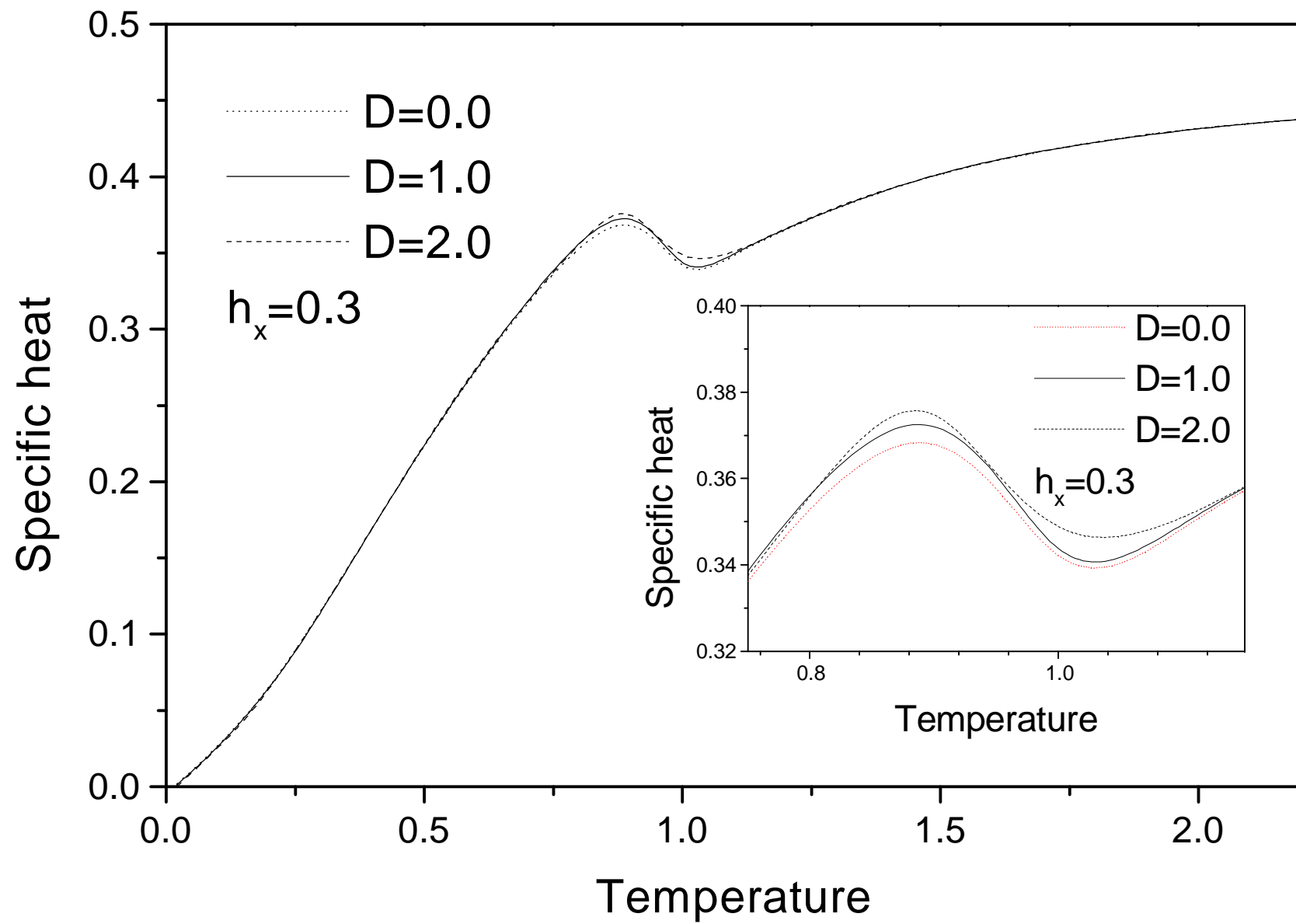


Fig.2 Xing, Su et al

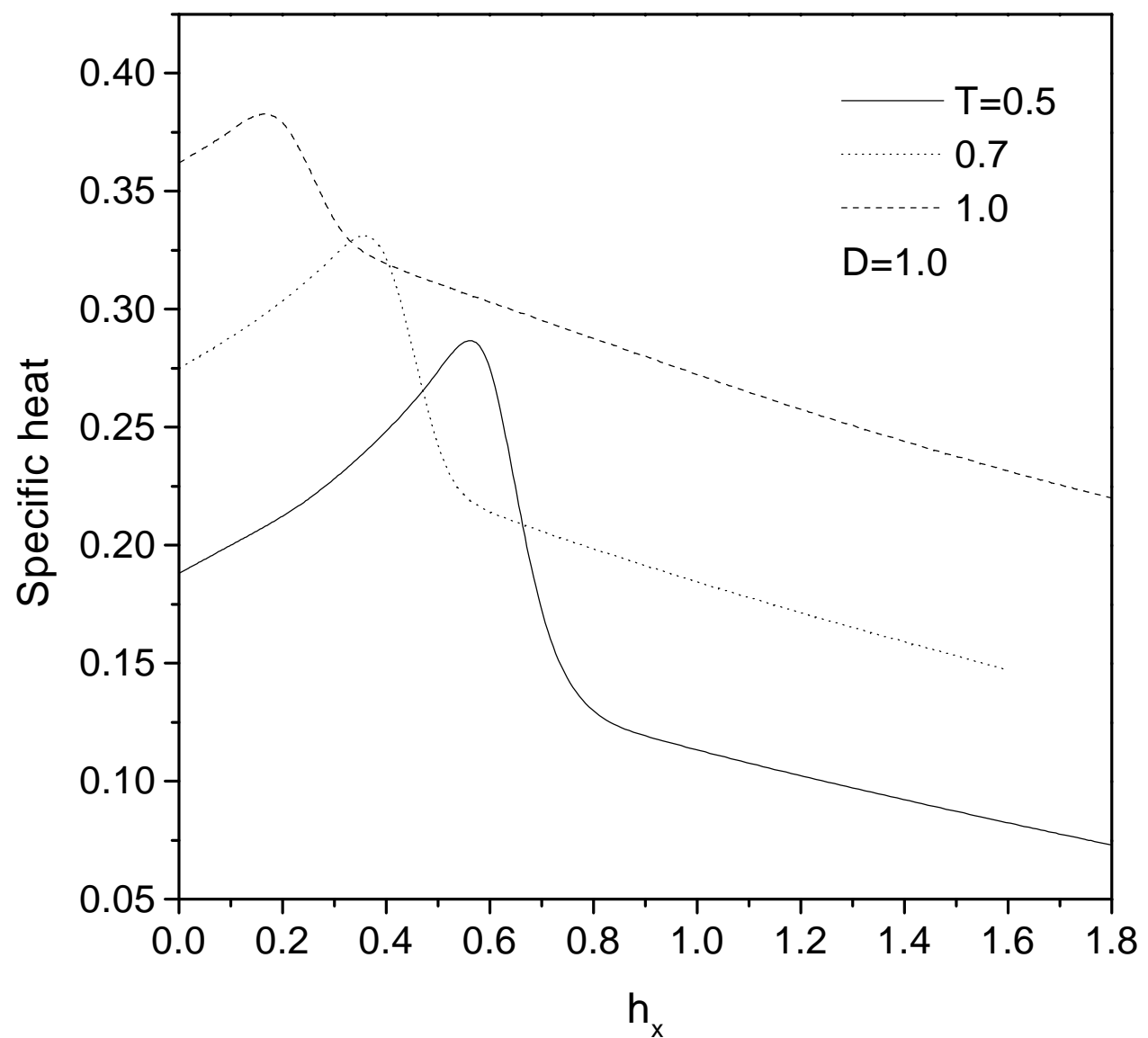


Fig.3 Xing, Su et al

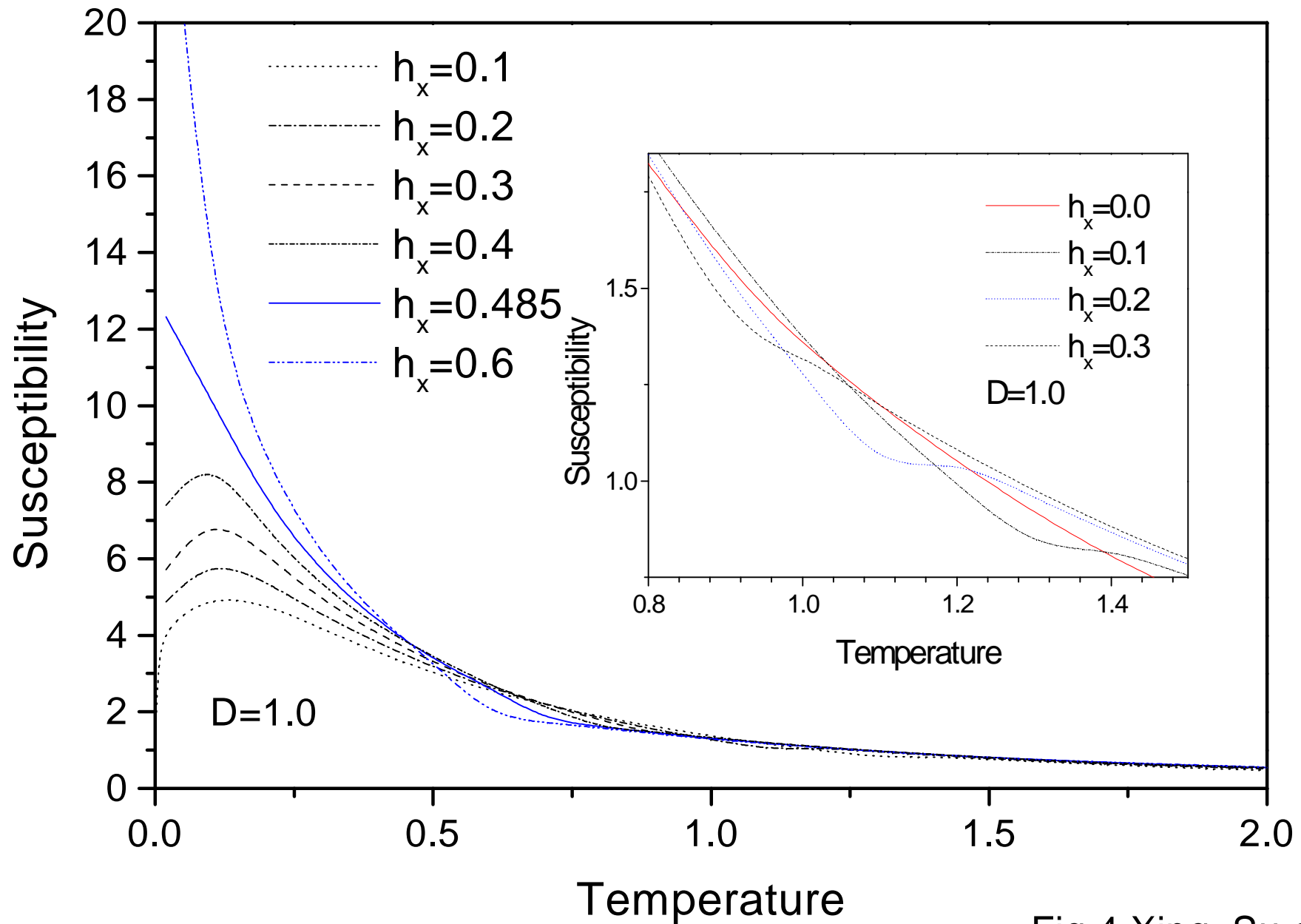


Fig.4 Xing, Su et al

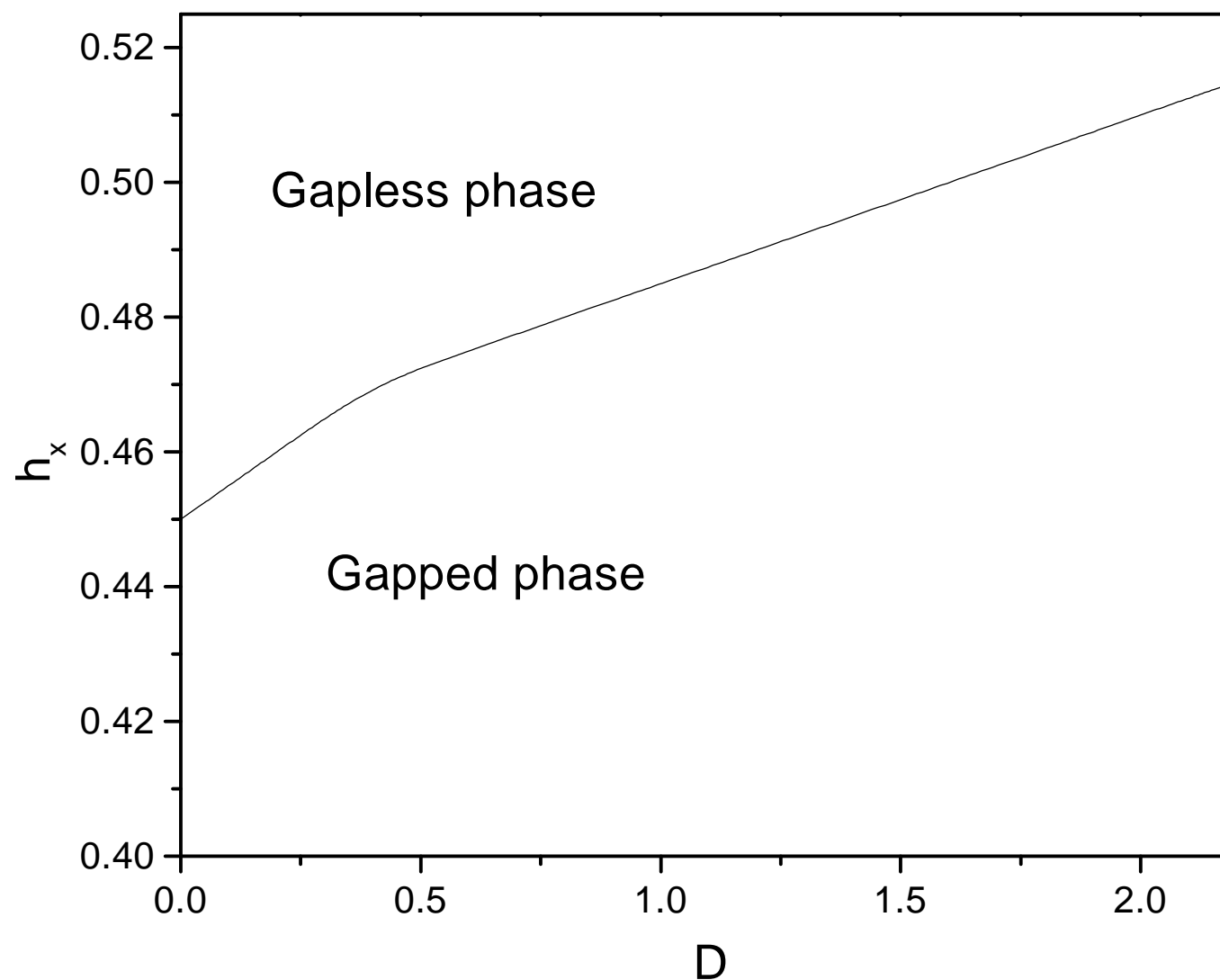


Fig.5 Xing, Su et al

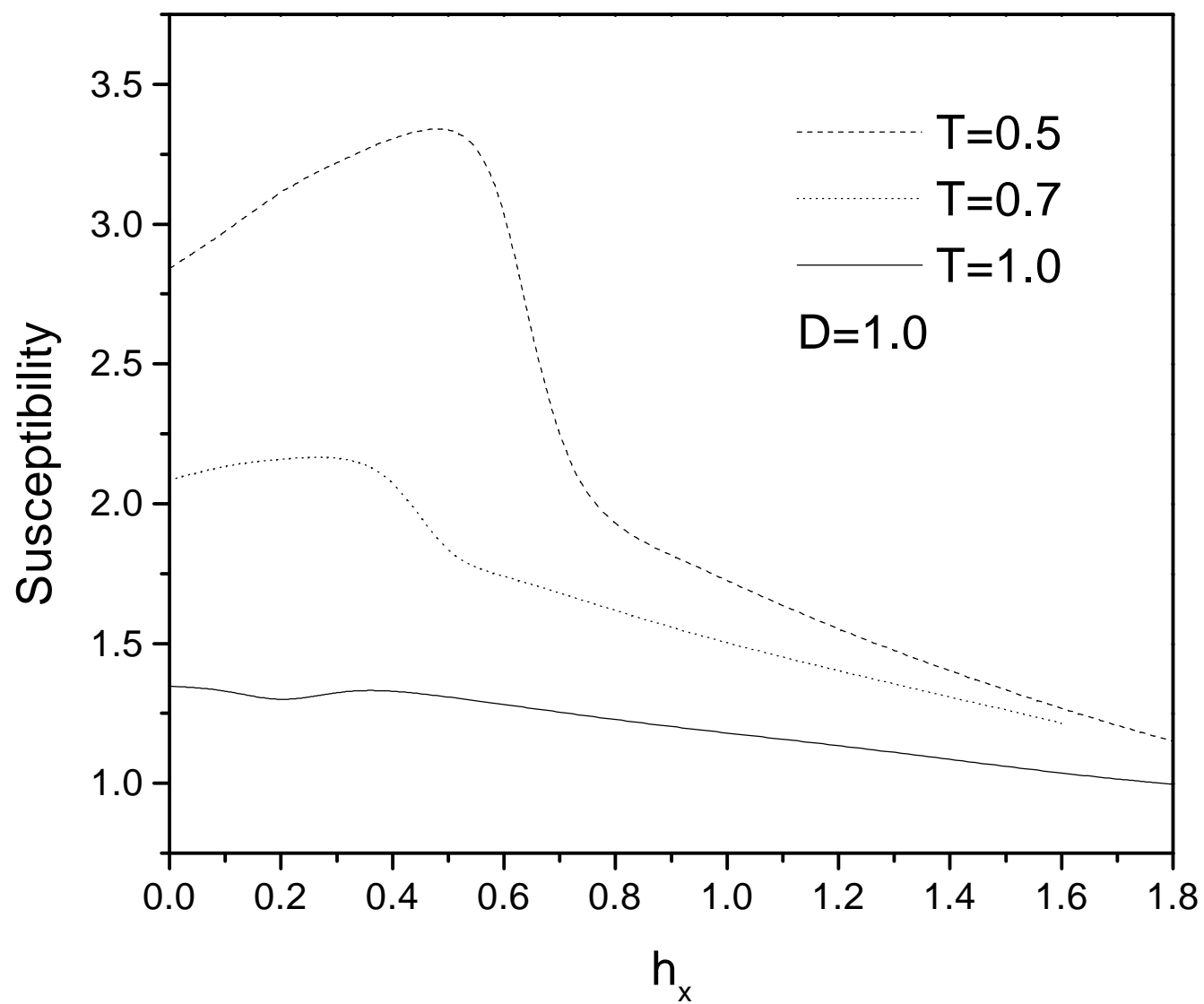


Fig.6 Xing, Su et al

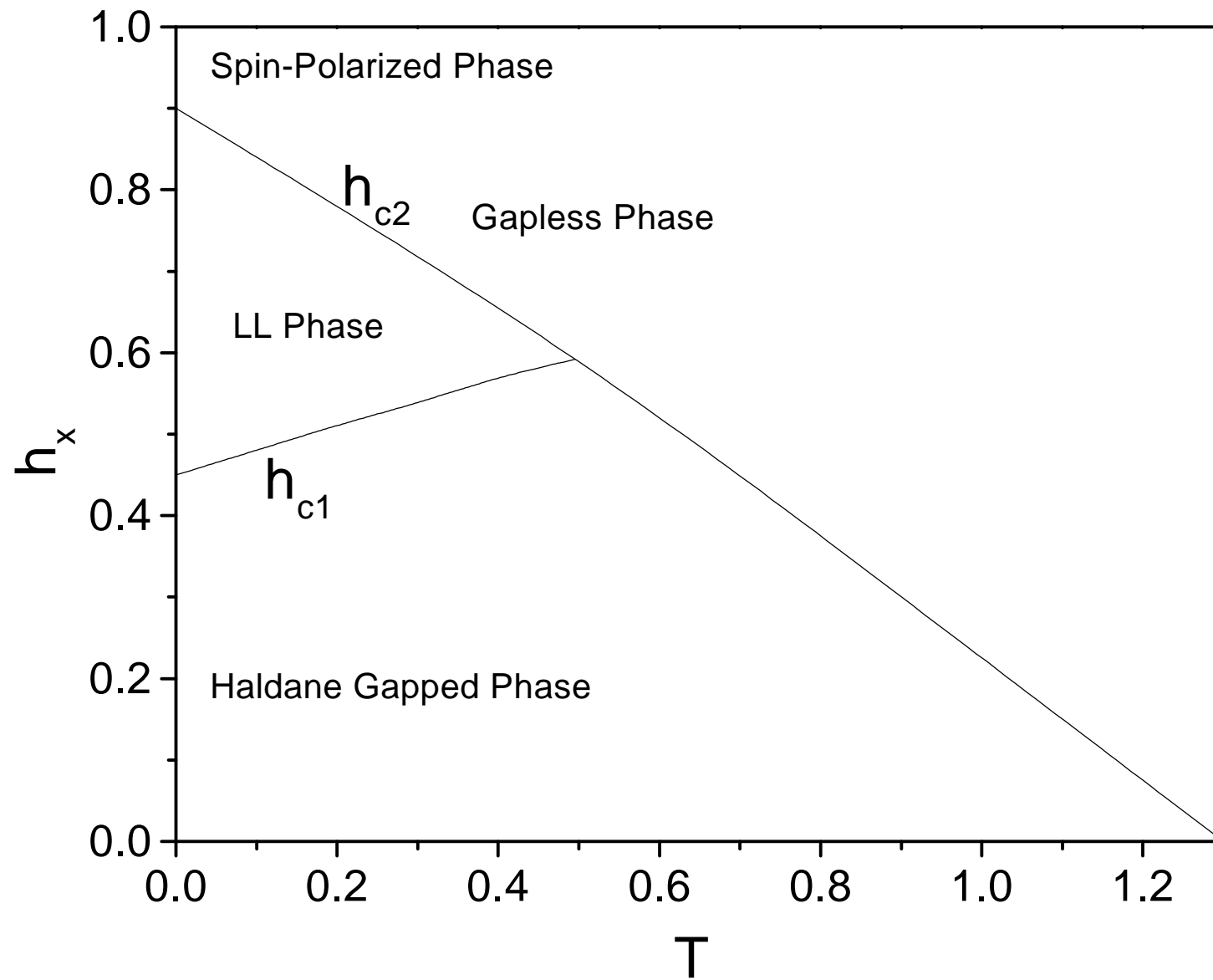


Fig.7 Xing, Su et al